Annals of Anatomy 226 (2019) 29–34

Contents lists available at ScienceDirect

Annals of Anatomy

journal homepage: www.elsevier.com/locate/aanat

Special issue research article

Anatomical analyses for maxillary sinus floor augmentation with a lateral approach: A cone beam computed tomography study☆

Shunsuke Kawakami[a], Daniele Botticelli[b,c,*], Yasushi Nakajima[a], Shigeru Sakuma[b], Shunsuke Baba[a]

[a] Department of Oral Implantology, Osaka Dental University, Osaka, Japan
[b] ARDEC Academy, Rimini, Italy
[c] DentalPro Academy, Milan, Italy

ARTICLE INFO

Article history:
Received 4 April 2019
Received in revised form 6 July 2019
Accepted 8 July 2019

Keywords:
Maxillary sinus
Cone beam computed tomography
Sinus septa
Posterior superior alveolar artery
Palatal–nasal recess

ABSTRACT

Background: Various anatomical references and structures should be analyzed prior approaching a surgery in the maxillary sinus. The objective of the present study was to evaluate the anatomical structures and references involved in sinus floor elevation with a lateral approach.
Materials and methods: Seventy-five patients planned for sinus floor elevation were included in the study. Eighty-eight maxillary sinuses were evaluated using cone beam computed tomographies (CBCTs). The nasal floor was used as main reference (X) and sinus mucosa width, bone crest height, palatal–nasal recess angle (PNR), sinus width at the level of the nasal floor, distance from the nasal floor to the base of the sinus (X–F), position of the posterior superior alveolar artery (PSAA height) and diameter (PSAA diameter), lateral bone wall width at 3 mm (LW 3 mm) and 9 mm (LW 9 mm) from the base of the sinus (F), patency of the ostium (OP), and presence and position of septa have been evaluated.
Results: The mean dimensions and standard deviations were the following: mucosa thickness was 2.0 ± 1.4 mm, bone crest height 2.8 ± 1.4 mm, distance X–F 8.3 ± 1.9 mm, PNR angle 135.5 ± 23.1, sinus width 12.6 ± 4.2 mm, X–F 8.3 ± 1.9 mm, PSAA height 14.4 ± 2.9 mm, PSAA diameter 1.1 ± 0.4 mm, LW 3 mm 1.5 ± 1.2, LW 9 mm 1.3 ± 0.6 mm, OP 1.9 ± 0.4 mm. Septa were present in 19.3% of the sinuses evaluated and were located mostly in the molar region.
Conclusions: In conclusion, the analysis of the CBCT before sinus floor elevation allows the identification of anatomical structures and references that might be used for the planning of the surgical approach, aiming to improve the outcome of the treatment and to avoid possible complications.

1. Introduction

Sinus floor augmentation procedures may be required for the rehabilitation of the posterior regions of the maxilla by means of implants, aiming to increase bone volume for implant installation. As all surgical procedures, sinus floor augmentation with a lateral approach presents technical difficulties and possible complications (Danesh-Sani et al., 2016). The most frequent intraoperative complication is the sinus mucosa perforation, while hemorrhagic events are less frequently reported (Stacchi et al., 2017). To reduce the incidence of possible complications, a cone beam computed tomography (CBCT) should be taken before performing the surgical procedures, aiming to evaluate the anatomy of the sinus (Danesh-Sani et al., 2016).

Various anatomical references and structures should be analyzed prior approaching a surgery in the maxillary sinus. The height of the residual bone crest (Cavalcanti et al., 2018; Lozano-Carrascal et al., 2017; Monje et al., 2014; Shanbhag et al., 2014; Tükel and Tatli, 2018), the thickness of the lateral sinus bone wall (Monje et al., 2014; Shanbhag et al., 2014; Danesh-Sani et al., 2017; Şimşek Kaya et al., 2019; Lim et al., 2017; Yang et al., 2012) and the angulation of the palatal–nasal recess (Chan et al., 2013; Niu et al., 2018) are important anatomical structures that might affect the complexity of the surgery. Moreover, the presence of septa (Şimşek Kaya et al., 2019; Tükel and Tatli, 2018; Ata-Ali et al., 2017; Lozano-Carrascal et al., 2017; Schriber et al., 2017; Maestre-Ferrín et al., 2010; Kim et al., 2006) contributes to increase the difficulties in the detachment of the Schneiderian membrane from the bone and might favor

☆ This paper belongs to the special issue "Applied Anatomy".

* Corresponding author at: ARDEC Academy, Ariminum Odontologica, Viale Giovanni Pascoli 67, 47923 Rimini, Italy.
E-mail address: daniele.botticelli@gmail.com (D. Botticelli).

https://doi.org/10.1016/j.aanat.2019.07.003
0940-9602/

perforations. Diameter and location of the intra-osseous anastomosis, that connects the posterior superior alveolar artery to the infraorbital artery, might have an important impact for possible hemorrhagic events (Lozano-Carrascal et al., 2017; Şimşek Kaya et al., 2019; Valente, 2016; Varela-Centelles et al., 2015; Testori et al., 2010; Mardinger et al., 2007; Solar et al., 1999). Moreover, the patency of the ostium, the thickness of the mucosa and the presence of abnormal structures in the sinus mucosa might affect the post-operative course.

It has been suggested to use the base of the nose as reference axes for analyses of the CBCTs images in both the coronal (*X* axis) and the lateral views (*Z* axis) (Kawakami et al., 2018, 2019). An accurate assessment of the various anatomical structures involved influence the surgical approach and might decrease the occurrence of complications.

Hence, the aim of the present study was to evaluate the anatomical structures and references involved in sinus floor elevation with a lateral approach.

2. Materials and methods

The protocol was approved by the Ethical Committee of the University Corporation Rafael Núñez, Cartagena de Indias, Colombia (protocol # CURN-01-2019). Informed consent was obtained from all participants. The present cross-sectional observational study followed the STROBE checklist.

2.1. Study population

Patients who underwent maxillary sinus augmentation for oral rehabilitation by means of implants were included in the study. The patients had to satisfy the following requisites: (i) to have a recent CBCT taken before the maxillary sinus augmentation; (ii) to be ≥21 years old; (iii) to have an edentulous region in the posterior maxilla; (iv) to have a height of the sinus floor ~4 mm or less; (v) to desire a prosthetic restoration using a fixed dental prosthesis supported by implants; (vi) to be in good general health; (vii) not to have any contraindications for oral surgical procedures; (viii) not being pregnant.

Patients who presented (i) a systemic disorder or were under (ii) chemotherapeutic or radiotherapeutic treatment or (iii) were smokers of >10 cigarettes/day were excluded from the study. Moreover, patients who referred with (iv) an acute or a chronic sinusitis or that (v) received a bone augmentation procedure in the region of interest were also excluded.

All patients were recruited and treated at the University Corporation Rafael Núñez, Cartagena de Indias (Colombia).

2.2. CBCT imaging procedures

The cone beam computed tomographies (CBCTs) were taken before the surgical treatment in a radiological center. A 3D Accuitomo 170 Tomograph (J Morita Corporation, Kyoto, Japan) was used.

2.3. CBCT imaging analyses

All radiographic assessments were carried out with the i-Dixel 2.0 software (J. Morita Corporation, Kyoto, Japan). As horizontal reference plane, the floor of the nose was chosen for both the coronal (X-axis; Fig. 1) and lateral views (Z-axis; Fig. 2). As vertical reference plane, a line crossing the anterior nasal spine and the nasal septum was used in the coronal view (Kawakami et al., 2018, 2019).

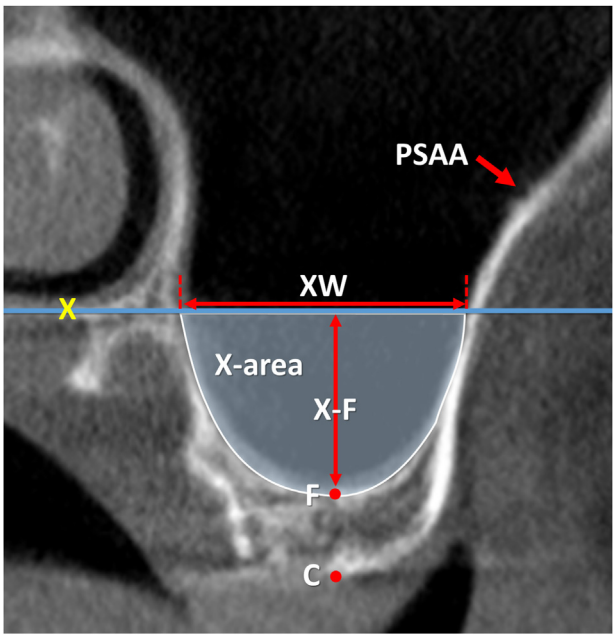

Fig. 1. Coronal view of a CBCT before sinus floor augmentation. X, line drawn following the floor of the nose; C, center of the bony crest; F, base of the sinus floor; A, anastomosis. X–F, nasal floor height; XW (sinus width), i.e. the distance evaluated on the line X between the two intersection points with the medial and lateral sinus bone walls. X-area, area delimited by the sinus bone walls and the line X.

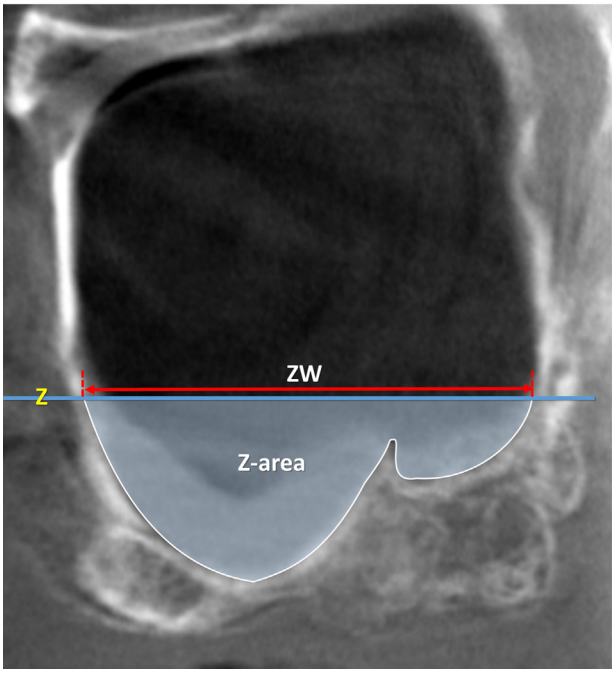

Fig. 2. Lateral view of a CBCT before sinus floor augmentation. Z, line drawn following the floor of the nose; ZW (sinus extension), i.e. the distance evaluated on the line Z between the two intersection points with the mesial and distal sinus bone walls. Z-area, area delimited by the sinus bone walls and the line Z.

2.4. Radiographic evaluations in the coronal view

The following landmarks were identified: bony crest center (C), sinus floor base (F), infra-osseous anastomosis (A), and center of the ostium (O) (Fig. 1).

The following parameters were assessed: mucosa thickness (MT), bone crest height (distance C–F), sinus height (distance X–F),

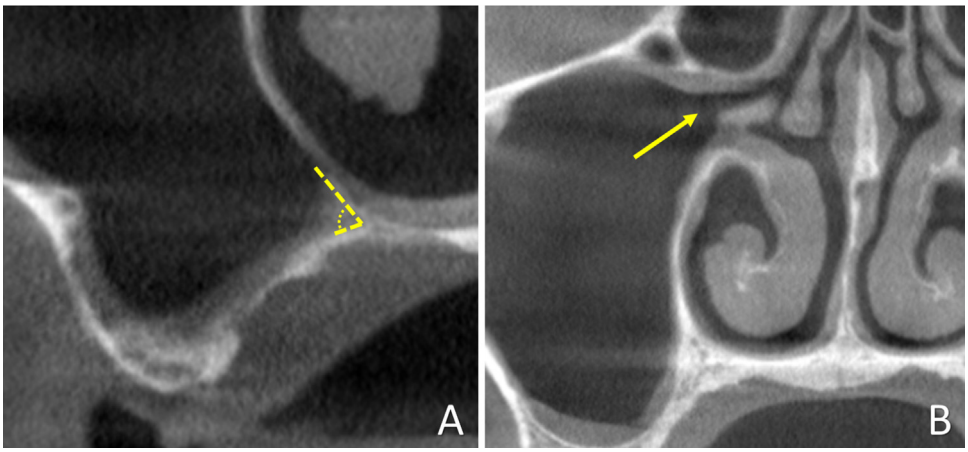

Fig. 3. (A) The yellow lines mark out the angle at the palatal–nasal recess. (B) The yellow arrow indicated the ostium. (For interpretation of the references to color in this figure legend, the reader is referred to the web version of this article.)

sinus width (XW; i.e. distance between the medial and lateral sinus bone walls on the X-axis), X-area (the area enclosed by the sinus bone walls and the X-axis), palatal–nasal recess height (PNR height, distance X–C), angle of the palatal–nasal recess (PNR angle; Fig. 3A). Moreover, the posterior superior alveolar artery (PSAA) distance from the bone crest (distance A–C, evaluated following the plane of the lateral sinus wall) and its diameter, the width of the lateral wall at 3 and 9 mm (LW3; LW9) from F, and the patency of the ostium (OP; Fig. 3B), were also evaluated.

2.5. Radiographic evaluations in the lateral view

The following references were used: the tip of the anterior nasal spine (NS) and the center of the ostium (O), as located in the coronal view.

The following parameters were assessed: sinus length (ZW; distance between the two intersection points with the mesial and distal sinus bone walls on the Z-axis) and area included between the bone walls and Z-axis (Fig. 2).

Moreover, the presence of septa within the sinus was evaluated using both lateral and axial views (Fig. 4A and B). Their height and location were recorded.

2.6. Data analysis

To reduce possible biases, all radiographic evaluations were performed twice by a well-trained assessor (KAAA, see Acknowledgements) with an intra-examiner coefficient $k > 0.8$ for all variables. Moreover, the use of well-defined references for all patients allowed the reproducibility of the measurements. Mean values were calculated for the two measurements. Mean values and standard deviations (SD) were subsequently calculated for each variable.

As explorative aim, data categorized for type of edentulism, sex, and age were provided.

3. Results

Eighty-eight sinuses of 75 patients, race mulatto, consecutively visited at the University Corporation Rafael Núñez of Cartagena de Indias, Colombia, from August 2015 to March 2018 were analyzed using CBCTs.

The mean age of the patients was 54.7 ± 9.5 years old, of which 47 were female and 28 were male (Table 1). All patients were non-smokers. Twenty-one patients were fully edentulous and fifty-four were partially edentulous. Forty-nine sinus evaluated were at the right side of the maxilla and 39 at the left side.

The evaluation in the CBCTs was performed mainly in the molar region (81 sites) while only few were in the premolar region (7 sites).

3.1. CBCT imaging evaluation

3.1.1. Coronal view

The sinus mucosa presented a thickness of 2.0 ± 1.4 mm (Table 2A). Thirty patients presented a thickness ≤1 mm, the thinner being 0.4 mm.

The bone crest height was 2.8 ± 1.4 mm, the shorter being 1.0 mm, while the distance between the X-axis and the sinus floor was 8.3 ± 1.9 mm. The total distance between the bone crest and the X-axis was 11.1 ± 2.6 mm, corresponding to the PNR height (X–C). The lowest values found were 6.2 mm. The palatal–nasal recess presented mean angles of 135.5 ± 23.1°. Only two were ≤90°, being 60° the most acute.

The width of the sinus, that represents the distance between the lateral and medial bone walls of the sinus evaluated on the X-axis, was 12.6 ± 4.2 mm. The area subjacent the X-axes in the coronal view was 80.6 ± 35.2 mm^2.

The PSAA was located 14.4 ± 2.9 mm above the bone crest, being the lowest distance 10.4 mm (Table 2B). The mean diameter of the PSAAs was 1.1 ± 0.4 mm. About 43% were <1 mm, 84% were <1.5 mm. Thirteen PSAA were found to be between 1.5 mm and 2 mm while only one presented a diameter of 2.2 mm.

The width of the lateral bone wall was 1.5 ± 1.2 mm and 1.3 ± 0.6 mm at 3 mm and 9 mm from the sinus floor, respectively, the highest values being 3.7 mm.

The mean patency of the ostium was 1.9 ± 0.4 mm, presenting a minimum diameter of 0.9 mm. Only one ostium presented a patency <1 mm, while most were included between 2 and 3 mm. Only two sinuses presented an ostium with a diameter larger than 3 mm.

Data categorized for type of edentulism, sex, and age are illustrated in Tables 4A and 4B.

3.1.2. Lateral view

The extension of the sinus on the Z-axis was 16.1 ± 2.6 mm while the area subjacent that Z-axis was 107.7 ± 36.2 mm^2 (Table 3). The distance between the anterior nasal spine and the anterior and posterior extension of the sinus was 22.5 ± 3.9 mm and 49.3 ± 5.9 mm, respectively. Septa were found in 17 cases out of 88. They were

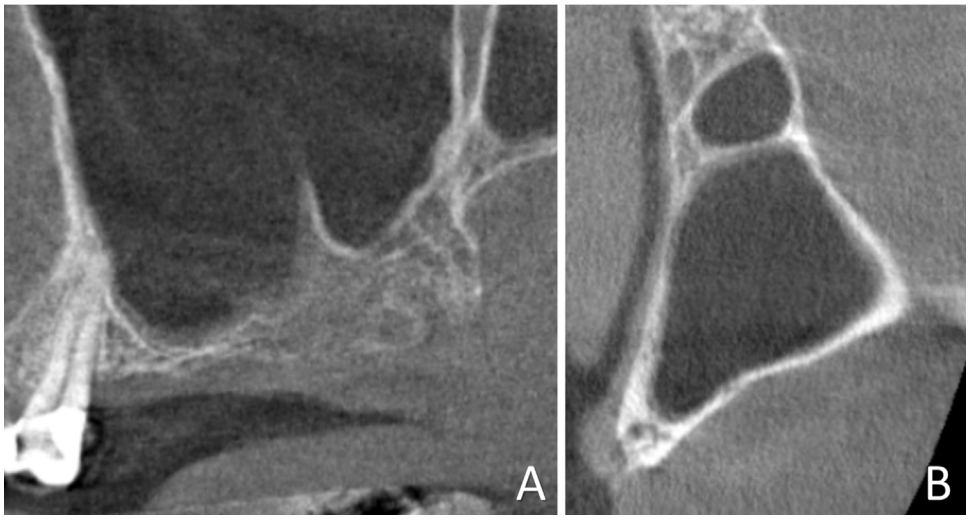

Fig. 4. Septum within the sinus evaluated using both lateral (A) and axial (B) views.

Table 1
Demographic and clinical data.

Sex	Age (years)	Smokers	Side	Regions evaluated
47 females28 males	54.7 ± 9.5	None	49 right, 39 left	7 premolars, 81 molars regions

Table 2A
Radiographic anatomical data in the coronal view. Data in millimeters or square millimeters for X-area.

	Mucosa thickness	Bone crest height (C–F)	Sinus height (X–F)	PNR height (X–C)	PNR angle	Sinus width (XW)	X-area
Mean values ± SD	2.0 ± 1.4	2.8 ± 1.4	8.3 ± 1.9	11.1 ± 2.6	135.5 ± 23.1	12.6 ± 4.2	80.6 ± 35.2
Median (25%; 75%)	1.8 (0.9; 3.3)	2.8 (1.5; 4.0)	7.5 (7.3; 9.6)	10.6 (9.1; 12.2)	136.4 (129.5; 150.0)	11.8 (9.9; 13.9)	72.8 (53.9; 100.0)

Table 2B
Radiographic anatomical data in the coronal view. Data in millimeters.

	PSAA height	PSAA diameter	LW 3 mm	LW 9 mm	OP
Mean values ± SD	14.4 ± 2.915.2 (13.0; 16.5)	1.1 ± 0.41.1 (0.7; 1.4)	1.5 ± 1.21.1 (0.7; 1.6)	1.3 ± 0.61.1 (0.9; 1.5)	1.9 ± 0.41.9 (1.7; 2.2)
Median (25%; 75%)					

Table 3
Radiographic anatomical data in the lateral view. Data in millimeters or square millimeters for Z-area.

	Sinus length	Anterior extension	Posterior extension	Septa height (n = 17)	Z-area
Mean values ± SD	16.1 ± 2.617.0 (16.3; 17.1)	22.5 ± 3.922.3 (19.6; 24.9)	49.3 ± 5.950.0 (46.6; 53.8)	7.0 ± 3.37.0 (5.8; 8.2)	107.7 ± 36.2
Median (25%; 75%)					104.7 (82.1; 137.9)

Table 4A
Radiographic anatomical data in the coronal view. Data in millimeters or square millimeters for X-area. Mean values ± standard deviation.

	Mucosa thickness	Bone crest height (C–F)	Sinus height (X–F)	PNR height (X–C)	PNR angle	Sinus width (XW)	X-area
Total edentulous	2.8 ± 3.6	3.1 ± 1.0	8.6 ± 1.7	11.7 ± 2.0	127.6 ± 18.8	14.8 ± 3.0	87.0 ± 27.4
Partial edentulous	3.2 ± 4.2	3.2 ± 1.3	9.9 ± 3.2	13.1 ± 3.1	132.7 ± 23.0	15.5 ± 3.8	100.3 ± 46.7
Females	3.2 ± 3.6	3.3 ± 1.3	9.8 ± 2.6	13.1 ± 2.6	132.2 ± 20.1	15.6 ± 2.9	101.6 ± 38.0
Male	2.9 ± 4.7	2.9 ± 1.2	9.1 ± 3.2	12.0 ± 3.1	129.6 ± 24.7	14.9 ± 4.5	93.0 ± 48.7
30–39 years	2.1 ± 2.1	3.5 ± 1.5	9.2 ± 2.8	12.8 ± 3.1	138.2 ± 16.1	14.7 ± 4.7	88.1 ± 34.9
40–49 years	3.4 ± 3.6	2.7 ± 1.0	10.3 ± 3.2	12.9 ± 3.3	136.1 ± 15.1	15.7 ± 1.2	110.5 ± 39.5
50–59 years	3.0 ± 3.4	3.2 ± 1.4	9.4 ± 3.5	12.5 ± 2.6	126.0 ± 23.8	15.6 ± 4.2	97.7 ± 45.8
≥60 years	3.2 ± 5.1	3.3 ± 1.1	9.4 ± 3.2	12.7 ± 2.9	132.6 ± 23.3	14.9 ± 3.5	95.0 ± 42.2

Table 4B
Radiographic anatomical data in the coronal view. Data in millimeters. Mean values ± standard deviation.

	PSAA height	PSAA diameter	LW 3 mm	LW 9 mm	OP
Total edentulous	16.8 ± 3.0	1.1 ± 0.3	1.2 ± 0.7	1.2 ± 0.6	2.0 ± 0.7
Partial edentulous	17.0 ± 3.4	1.1 ± 0.4	1.4 ± 0.7	1.2 ± 0.5	1.7 ± 0.4
Females	17.4 ± 3.3	1.0 ± 0.4	1.3 ± 0.7	1.2 ± 0.5	1.8 ± 0.4
Male	16.3 ± 3.1	1.2 ± 0.4	1.3 ± 0.7	1.3 ± 0.6	1.8 ± 0.7
30–39 years	15.9 ± 4.9	1.4 ± 0.5	1.4 ± 0.5	1.6 ± 0.5	1.7 ± 0.4
40–49 years	18.7 ± 3.9	0.9 ± 0.4	1.4 ± 0.6	1.1 ± 0.3	1.8 ± 0.5
50–59 years	16.7 ± 2.8	1.0 ± 0.4	1.3 ± 0.6	1.2 ± 0.4	1.9 ± 0.4
≥60 years	16.5 ± 2.7	1.2 ± 0.4	1.3 ± 0.8	1.3 ± 0.7	1.8 ± 0.7

located mostly in the second molar region and presented a height from 3.1 mm to 10 mm.

4. Discussion

In the present study, the sinus mucosa presented a mean width of 2.0 mm and about 73% was ≤3 mm. This is in agreement with another study that analyzed three-hundred CBCTs of patients scheduled for implant surgery (Lozano-Carrascal et al., 2017). In that study, the mean sinus mucosa thickness was 2 mm, of which about 70% was ≤3 mm. The measurements of the sinus mucosa in the present study were made in the regions planned for implant installation. However, it has been shown that the sinus mucosa exhibits a wide range of thickness in the various regions of the same sinus (Janner et al., 2011).

In the present study, the height of the bone crest and the distance between the floor of the sinus and the X-axis was evaluated. The X-axis was placed at the level of the nasal floor that is located roughly at the level of the palatal–nasal recess (PNR). Consequently, the distance between the bone crest and the X-axis represents a clinical reference that provides the location of the PNR. The mean X–C distance was 11.1 mm and in 72 sinuses (83.7%) it was <15 mm. The distance X–C of 15 mm was classified as a risk factor together an angle <90° formed by the nasal and palatal bone walls at the PNR (Chan et al., 2013). This risk factor may be related to the elevation of the sinus obtained to install an implant of adequate length and the difficulties that may be encountered to elevate the sinus mucosa on the palatal aspect, cranially to the PNR, if the angle is <90°. In the present study, only two sinuses had a PNR angle <90°. One sinus had an X–C height >15 mm so that this site could be excluded from the risk category. The second sinus presented a X–C of 14.4 mm so that, accordingly with this classification, it should be included in the risk category. However, to classify a sinus as risky, the length of the implant selected by the clinician should be taken into consideration. In a systematic review with meta-analyses, the outcomes after three years between short implants and standard implants installed in augmented sinuses were evaluated (Nielsen et al., 2019). The minimum length of the standard implants used at the augmented sinuses was 10 mm. This, in turn, means that the height from the bone crest and the top of the augmented sites after healing should exceed at least this dimension.

The resorptive properties of the biomaterial used as filler have also to be considered because they will affect the final dimensions of the augmented sites. In the present study, 17 (19.8%) sinuses presented an X–C height <10 mm. This means that, in these sites, the elevation of the sinus mucosa at the palatal aspect most likely will exceed cranially the limit of the PNR. If the PNR angle is acute (≤90°), in might be difficult to detach the sinus mucosa from the bone. In the present study, out of the 17 sinuses (19.3%) with an X–C <10 mm, only two presented an angle ≤90°, one exhibited an angle of ∼91°, while the remaining fourteen sinuses had angles ≥129°. This latter PNR angle might allow a relatively easily elevation of the sinus mucosa at the palatal aspect so that only three sinuses should be considered at risk in the present set of sinuses.

Another aspect that should be considered is that the sinus floor elevation using a lateral access will result in a dome shape, meaning that the middle region of the augmented sites will be more elevated in respect of the palatal and lateral aspects (Kawakami et al., 2018, 2019). In clinical studies in which a collagenated cortico-cancellous porcine bone, a difference in height between the medial and the middle region of the augmented sinus was 3.8–5.3 mm one week after surgery (Kawakami et al., 2018, 2019). After nine months of healing, the difference decreased to 1.5–3.3 mm. This, in turn, means that this difference of ∼2 mm might be considered in the calculation for the selection of the implant length.

From a clinical point of view, in the case of a short X–C (<10) and a PNR angle <90°, it might be difficult to elevate the sinus mucosa cranially to the PNR. This will result in a lower exposition of the palatal bone wall into the elevated region. As the bone walls are the main source of newly formed bone (Scala et al., 2010, 2012; Caneva et al., 2017; Iida et al., 2017; Omori et al., 2018; Masuda et al., 2019), this may affect the healing from the palatal aspect. At the lateral aspect, the dimensions of the antrostomy performed on the lateral wall may also affect the healing, given that the larger the antrostomy, the lower the source of new bone (Kawakami et al., 2019). Moreover, the position of the antrostomy as well may influence the healing, so that preparing the lower border of the osteotomy cranially to the sinus floor will provide a self-contained region included between the lateral and medial bone walls (Kawakami et al., 2018).

The width of the sinus at the level of the X-axis may complicate the surgical procedures, especially when its dimension is large. In the present report, in six sinuses, the sinus width was >2 mm. This condition may require widening the antrostomy to get an improved access to the palatal aspect.

The position and dimension of the posterior superior alveolar artery (PSAA) may influence the position and dimensions of the antrostomy. It has been reported that severing PSAA with larger diameter may produce conspicuous bleeding that may require a surgical procedure to stop the hemorrhage (Testori et al., 2010). Several studies reported diameters of the PSAA and the distance between anastomosis and bony crest. A radiological study performed on 208 CT images found that 6.7% of the anastomosis presented a diameter >2 mm (Mardinger et al., 2007). Moreover, in a study on cadavers, the mean distance between the PSAA and the bone crest was about 19 mm, even though lower distances, such as 8 mm, have been reported (Danesh-Sani et al., 2016). In the present study, the mean distance of the PSAA from the bony crest was 14.9 mm, with a minimum distance of 10.4 mm. In the presence of such short distance, the antrostomy might be located at the level of the PSAA and the diameter of the artery has to be considered because the risk of important hemorrhagic event is high. In fact, in the present study, 11 sinuses presented a PSAA >1.5 mm of diameter and in one sinus was >2 mm. In such cases, the use of piezo surgical or sonic instruments is highly recommended (Masuda et al., 2019; Kawakami et al., 2018, 2019; Agabiti and Botticelli, 2016, 2017; Vercellotti et al., 2001).

The presence of septa has also to be considered in the analysis of a CBCT. In the present experiment, septa were present in 17 sinuses (19.3%), with a height included between 3.1 and 10.0 mm. Other studies reported higher percentages, such as 66.5% (Bornstein et al., 2016) or 35.1% (Şimşek Kaya et al., 2019), or similar to the present study, such a 26.5% (Kim et al., 2006) and 20.6% (Lozano-Carrascal et al., 2017). A systematic review analyzed 11 papers and reported percentages of presence of septa between 13% and 35.3%. The septa have been associated with higher risk of perforation of the sinus mucosa during the surgical procedures (Tükel and Tatli, 2018).

Finally, the patency of the ostium was also evaluated, and the majority showed a patent of ≤2 mm. Obstruction of the ostium should be verified prior the surgery to avoid possible post-surgical complications (Shanbhag et al., 2014).

Data categorized for type of edentulism, sex, and age have been included in the present study. However, no major differences were seen among categories.

The main limitation of the present study is the lack of information about the outcomes of the treatment that are however reported elsewhere.

Clinically, it might be suggested to achieve as much as possible of the bone walls exposed within the elevated space to increase the source of newly formed bone. This, in turn, means that the position and the dimension of the antrostomy as well as a proper sinus

mucosa elevation at the palatal aspect are of great importance. The angle of the palatal–nasal recess, the position of the posterior superior alveolar artery and the presence of septa might influence the surgical approach. The clinicians should identify all the anatomical structures on CBCTs before performing the surgical procedures.

In conclusion, the analysis of the CBCT before sinus floor elevation allows the identification of anatomical structures and references that might be used for the planning of the surgical approach, aiming to improve the outcome of the treatment and to avoid possible complications.

Acknowledgements

ARDEC Academy, Ariminum Odontologica s.r.l., Rimini, Italy provided the economical and scientific support for the experiment. The authors thank the support provided by Dr. Mauro Ferri for the clinical management of the patients and Dr. Karol Alí Apaza Alccayhuaman (KAAA) for the time spent for the analyses on the CBCT.

References

Agabiti, I., Botticelli, D., 2016. Transcrestal sinus floor elevation performed twice with collagen sponges and using a sonic instrument. J. Oral Sci. Rehabil. 2 (1), 40–47.

Agabiti, I., Botticelli, D., 2017. Two-stage ridge split at narrow alveolar mandibular bone ridges. J. Oral Maxillofac. Surg. 75 (10), 2115, e1-2115.e12.

Ata-Ali, J., Diago-Vilalta, J.V., Melo, M., Bagán, L., Soldini, M.C., Di-Nardo, C., Ata-Ali, F., Mañes-Ferrer, J.F., 2017. What is the frequency of anatomical variations and pathological findings in maxillary sinuses among patients subjected to maxillofacial cone beam computed tomography? A systematic review. Med. Oral Patol. Oral Cir. Bucal. 22 (4), e400–e409.

Bornstein, M.M., Seiffert, C., Maestre-Ferrín, L., Fodich, I., Jacobs, R., Buser, D., von Arx, T., 2016. An analysis of frequency, morphology, and locations of maxillary sinus septa using cone beam computed tomography. Int. J. Oral Maxillofac. Implants 31 (2), 207–280.

Caneva, M., Lang, N.P., Garcia Rangel, I.J., Ferreira, S., Caneva, M., De Santis, E., Botticelli, D., 2017. Sinus mucosa elevation using Bio-Oss(®) or Gingistat(®) collagen sponge: an experimental study in rabbits. Clin. Oral Implants Res. 28 (7), e21–e30.

Cavalcanti, M.C., Guirado, T.E., Sapata, V.M., Costa, C., Pannuti, C.M., Jung, R.E., César Neto, J.B., 2018. Maxillary sinus floor pneumatization and alveolar ridge resorption after tooth loss: a cross-sectional study. Braz. Oral Res. 6 (32), e64.

Chan, H.L., Monje, A., Suarez, F., Benavides, E., Wang, H.L., 2013. Palatonasal recess on medial wall of the maxillary sinus and clinical implications for sinus augmentation via lateral window approach. J. Periodontol. 84 (8), 1087–1093.

Danesh-Sani, S.A., Loomer, P.M., Wallace, S.S., 2016. A comprehensive clinical review of maxillary sinus floor elevation: anatomy, techniques, biomaterials and complications. Br. J. Oral Maxillofac. Surg. 54 (7), 724–730.

Danesh-Sani, S.A., Movahed, A., ElChaar, E.S., Chong Chan, K., Amintavakoli, N., 2017. Radiographic evaluation of maxillary sinus lateral wall and posterior superior alveolar artery anatomy: a cone-beam computed tomographic study. Clin. Implant Dent. Relat. Res. 19 (1), 151–160.

Iida, T., Carneiro Martins Neto, E., Botticelli, D., Apaza Alccayhuaman, K.A., Lang, N.P., Xavier, S.P., 2017. Influence of a collagen membrane positioned subjacent the sinus mucosa following the elevation of the maxillary sinus. A histomorphometric study in rabbits. Clin. Oral Implants Res. 28 (12), 1567–1576.

Janner, S.F., Caversaccio, M.D., Dubach, P., Sendi, P., Buser, D., Bornstein, M.M., 2011. Characteristics and dimensions of the Schneiderian membrane: a radiographic analysis using cone beam computed tomography in patients referred for dental implant surgery in the posterior maxilla. Clin. Oral Implants Res. 22 (12), 1446–1453.

Kawakami, S., Lang, N.P., Ferri, M., Apaza Alccayhuaman, K.A., Botticelli, D., 2019. Influence of the height of the antrostomy in sinus floor elevation assessed by cone beam computed tomography – a randomized clinical trial. Int. J. Oral Maxillofac. Implants 34 (1), 223–232.

Kawakami, S., Lang, N.P., Iida, T., Ferri, M., Apaza Alccayhuaman, K.A., Botticelli, D., 2018. Influence of the position of the antrostomy in sinus floor elevation assessed with cone-beam computed tomography: a randomized clinical trial. J. Investig. Clin. Dent. 9 (4), e12362.

Kim, M.J., Jung, U.W., Kim, C.S., Kim, K.D., Choi, S.H., Kim, C.K., Cho, K.S., 2006. Maxillary sinus septa: prevalence, height, location, and morphology. A reformatted computed tomography scan analysis. J. Periodontol. 77 (5), 903–908.

Lim, E.L., Ngeow, W.C., Lim, D., 2017. The implications of different lateral wall thicknesses on surgical access to the maxillary sinus. Braz. Oral Res. 27 (31), e97.

Lozano-Carrascal, N., Salomó-Coll, O., Gehrke, S.A., Calvo-Guirado, J.L., Hernández-Alfaro, F., Gargallo-Albiol, J., 2017. Radiological evaluation of maxillary sinus anatomy: a cross-sectional study of 300 patients. Ann. Anat. 214, 1–8.

Maestre-Ferrín, L., Galán-Gil, S., Rubio-Serrano, M., Peñarrocha-Diago, M., Peñarrocha-Oltra, D., 2010. Maxillary sinus septa: a systematic review. Med. Oral Patol. Oral Cir. Bucal. 1 15 (2), e383–e386.

Mardinger, O., Abba, M., Hirshberg, A., Schwartz-Arad, D., 2007. Prevalence, diameter and course of the maxillary intraosseous vascular canal with relation to sinus augmentation procedure: a radiographic study. Int. J. Oral Maxillofac. Surg. 36, 735–738.

Masuda, K., Silva, E.R., Botticelli, D., Apaza Alccayhuaman, K.A., Xavier, S.P., 2019. Antrostomy preparation for maxillary sinus floor augmentation using drills or a sonic instrument: a microcomputed tomography and histomorphometric study in rabbits. Int. J. Oral Maxillofac. Implants, Epub ahead of print.

Monje, A., Catena, A., Monje, F., Gonzalez-García, R., Galindo-Moreno, P., Suarez, F., Wang, H.L., 2014. Maxillary sinus lateral wall thickness and morphologic patterns in the atrophic posterior maxilla. J. Periodontol. 85 (5), 676–682.

Nielsen, H.B., Schou, S., Isidor, F., Christensen, A.E., Starch-Jensen, T., 2019. Short implants (≤8 mm) compared to standard length implants (>8 mm) in conjunction with maxillary sinus floor augmentation: a systematic review and meta-analysis. Int. J. Oral Maxillofac. Surg. 48 (2), 239–249.

Niu, L., Wang, J., Yu, H., Quip, L., 2018. New classification of maxillary sinus contours and its relation to sinus floor elevation surgery. Clin. Implant Dent. Relat. Res. 20 (4), 493–500.

Omori, Y., Silva, R.E., Botticelli, D., Apaza Alccayhuaman, K.A., Lang, N.P., Xavier, S.P., 2018. Reposition of the bone plate over the antrostomy in maxillary sinus augmentation: a histomorphometric study in rabbits. Clin. Oral Implants Res. 29 (8), 821–834.

Scala, A., Botticelli, D., Freda, R.S., Garcia Rangel Jr., I., America de Oliveira, J., Lang, N.P., 2012. Lack of influence of the Schneiderian membrane in forming new bone apical to implants simultaneously installed with sinus floor elevation: an experimental study in monkeys. Clin. Oral Implants Res. 23 (2), 175–181.

Scala, A., Botticelli, D., Rangel Jr., I.G., de Oliveira, J.A., Okamoto, R., Lang, N.P., 2010. Early healing after elevation of the maxillary sinus floor applying a lateral access: a histological study in monkeys. Clin. Oral Implants Res. 21 (12), 1320–1326.

Schriber, M., von Arx, T., Sendi, P., Jacobs, R., Suter, V.G., Bornstein, M.M., 2017. Evaluating maxillary sinus septa using cone beam computed tomography: is there a difference in frequency and type between the dentate and edentulous posterior maxilla? Int. J. Oral Maxillofac. Implants 32 (6), 1324–1332.

Shanbhag, S., Karnik, P., Shirke, P., Shanbhag, V., 2014. Cone-beam computed tomographic analysis of sinus membrane thickness, ostium patency, and residual ridge heights in the posterior maxilla: implications for sinus floor elevation. Clin. Oral Implants Res. 25 (6), 755–760.

Şimşek Kaya, G., Daltaban, Ö., Kaya, M., Kocabalkan, B., Sindel, A., Akdağ, M., 2019. The potential clinical relevance of anatomical structures and variations of the maxillary sinus for planned sinus floor elevation procedures: a retrospective cone beam computed tomography study. Clin. Implant Dent. Relat. Res. 21 (Feb (1)), 114–121.

Solar, P., Geyerhofer, U., Traxler, H., Windisch, A., Ulm, C., Watzek, G., 1999. Blood supply to the maxillary sinus relevant to sinus floor elevation procedures. Clin. Oral Implants Res. 10, 34–44.

Stacchi, C., Andolsek, F., Berton, F., Perinetti, G., Navarra, C.O., Di Lenarda, R., 2017. Intraoperative complications during sinus floor elevation with lateral approach: a systematic review. Int. J. Oral Maxillofac. Implants 32 (3), e107–e118.

Testori, T., Rosano, G., Taschieri, S., Del Fabbro, M., 2010. Ligation of an unusually large vessel during maxillary sinus floor augmentation. A case report. Eur. J. Oral Implantol. 3 (3), 255–258.

Tükel, H.C., Tatli, U., 2018. Risk factors and clinical outcomes of sinus membrane perforation during lateral window sinus lifting: analysis of 120 patients. Int. J. Oral Maxillofac. Surg. 47 (9), 1189–1194.

Valente, N.A., 2016. Anatomical considerations on the alveolar antral artery as related to the sinus augmentation surgical procedure. Clin. Implant Dent. Relat. Res. 18 (5), 1042–1050.

Varela-Centelles, P., Loira-Gago, M., Seoane-Romero, J.M., Takkouche, B., Monteiro, L., Seoane, J., 2015. Detection of the posterior superior alveolar artery in the lateral sinus wall using computed tomography/cone beam computed tomography: a prevalence meta-analysis study and systematic review. Int. J. Oral Maxillofac. Surg. 44 (11), 1405–1410.

Vercellotti, T., De Paoli, S., Nevins, M., 2001. The piezoelectric bony window osteotomy and sinus membrane elevation: introduction of a new technique for simplification of the sinus augmentation procedure. Int. J. Periodontics Restorative Dent. 21 (6), 561–567.

Yang, S.M., Park, S.I., Kye, S.B., Shin, S.Y., 2012. Computed tomographic assessment of maxillary sinus wall thickness in edentulous patients. J. Oral Rehabil. 39 (6), 421–428.